Hydration, Structure, and Superconductivity of $KOs_2O_6 \cdot nH_2O$

Rosa Galati,[†] Charles Simon,[†] Christopher S. Knee,[‡] Paul F. Henry,[§] Brian D. Rainford,[△] and Mark T. Weller*,[†]

School of Chemistry and School of Physics, University of Southampton, Southampton SO17 1BJ, U.K., Department of Chemistry, University of Gothenburg, SE-412 96 Sweden, and Institut Laue Langevin, 6, rue Jules Horowitz, BP 156X, 38042 Grenoble Cedex 9, France

Received October 15, 2007. Revised Manuscript Received November 21, 2007

In moist air or by contact with water during washing, KOs_2O_6 absorbs water molecules into the structure to produce $KOs_2O_6 \cdot nH_2O$, $0 < n < 0.1$. This water is reversibly lost on heating above ~430 K in flowing or static gas environments. Variable temperature powder neutron and X-ray diffraction show that an increase in lattice parameter occurs when water enters the pyrochlore structure and the water molecules are located in the α cages displacing a portion of the potassium ions to adjacent sites. On removing water the lattice parameter and structure revert to those of the normal β-pyrochlore crystallographic description. Hydration has the effect of reducing the onset of superconducting behavior from a critical temperature of 10.25 K in fully dry KOs_2O_6 to 9.75 K in $KOs_2O_6 \cdot 0.1H_2O$.

Introduction

Transition metal containing complex oxides adopting the pyrochlore structure demonstrate a wide range of physical phenomena such as colossal magnetoresistance, metal−insulator transitions, ferroelectric behaviors, and geometrical magnetic frustration.[1,2] In 2001, $Cd_2Re_2O_7$ was reported as the first pyrochlore superconductor with $T_c = 1.4$ K.[3–5] More recently a new family of superconductors, AOs_2O_6 (A = Cs, Rb, K), adopting the β-pyrochlore structure, has been discovered with reported T_c's of 3.6 K, 6.3 K, and 9.6 K respectively.[6–8] In the α-pyrochlore $A_2B_2O_6O'$ (normally written $A_2B_2O_7$), BO_6 octahedra form the pyrochlore framework with an interpenetrating A_2O' sublattice generating a 2O′ (short) + 6O (long) coordination around the A-type cations. The structure is described in the space group $Fd\bar{3}m$ with A, B, O, and O′ on the 16d, 16c, 48f, and 8b positions, respectively. In the β-pyrochlore structure, the A cation is shifted from the 16d to the 8b position, replacing O′, while the BO_6 framework remains unchanged, Figure 1. Recent structural work on these β-pyrochlores has concentrated on KOs_2O_6, with two groups proposing different crystal structures from single crystal X-ray data. Schuck et al.[9,10] have stated that at room temperature and between 100 and 400 K their data shows additional reflections which violate $Fd\bar{3}m$ symmetry and suggest a symmetry reduction to $F\bar{4}3m$. This is in contrast to Yamaura et al.[11] who found no extra reflections in their data collected between 5 and 300 K (with only partial information collected below 100 K in oscillation photographs) and concluded that the structure is best described in $Fd\bar{3}m$. Both publications demonstrate that the atomic displacement parameter (ADP) of the A-type cation, potassium, at room temperature is unusually large when compared to those of other ions. These observations agree with the band structure calculations of Kuneš et al. where an instability in the optic mode of the K^+ ion was found to result in the "rattling" behavior.[12,13] Yamaura et al.[11] also state that

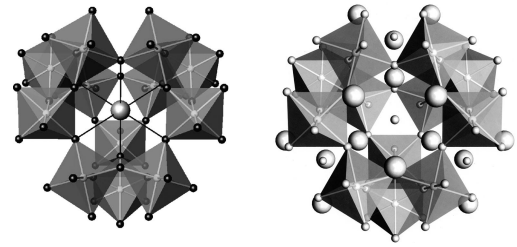

Figure 1. The β-pyrochlore (left) and α-pyrochlore (right) structures as viewed down the (111) direction and centered on (0.375, 0.375, 0.375). For KOs_2O_6, OsO_6 octahedra are shown shaded gray, oxygen as small pale gray spheres, and potassium as large gray spheres.

* Corresponding author. E-mail: mtw@soton.ac.uk.
† School of Chemistry, University of Southampton.
‡ University of Gothenburg.
§ Institut Laue Langevin.
△ School of Physics, University of Southampton.

(1) Subramanian, M. A.; Aravamudan, G.; Subba Rao, G. V. *Prog. Solid State Chem.* **1983**, *15*, 55.
(2) Greedan, J. E. *J. Mater. Chem.* **2001**, *11*, 37.
(3) Sakai, H.; Yoshimura, K.; Ohno, H.; Kato, H.; Kambe, S.; Walstedt, R. E.; Matsuda, T. D.; Haga, Y.; Onuki, Y. *J. Phys., Condens. Matter* **2001**, *13*, L785.
(4) Hanawa, M.; Muraoka, Y.; Tayama, T.; Sakakibara, T.; Yamaura, J.; Hiroi, Z. *Phys. Rev. Lett.* **2001**, *87*, 187001.
(5) Jin, R.; He, J.; McCall, S.; Alexander, C. S.; Drymiotis, F.; Mandrus, D. *Phys. Rev. B: Condens. Matter* **2001**, *64*, 180503.
(6) Yonezawa, S.; Muraoka, Y.; Hiroi, Z. *J. Phys. Soc. Jpn.* **2004**, *73*, 1655.
(7) Yonezawa, S.; Muraoka, Y.; Matsushita, Y.; Hiroi, Z. *J. Phys. Soc. Jpn.* **2004**, *73*, 819.
(8) Yonezawa, S.; Muraoka, Y.; Matsushita, Y.; Hiroi, Z. *J. Phys., Condens. Matter* **2004**, *16*, L9.
(9) Schuck, G.; Kazakov, S. M.; Rogacki, K.; Zhigadlo, N. D.; Karpinski, J. *Phys. Rev. B, Condens. Matter* **2006**, *73*, 144506.
(10) Schuck, G.; Karpinski, J.; Bukowski, Z.; Chernyshov, D. Temperature dependent structural studies of beta-pyrochlore KOs_2O_6 single crystals. Presented at *Jahrestagung der Deutsche Gesellschaft für Kristallographie*, March 5–9, 2007, Bremen, Germany.
(11) Yamaura, J. I.; Yonezawa, S.; Muraoka, Y.; Hiroi, Z. *J. Solid State Chem.* **2006**, *179*, 336.
(12) Kuneš, J.; Jeong, T.; Pickett, W. E. *Phys. Rev. B: Condens. Matter* **2004**, *70*, 174510.

10.1021/cm702972c CCC: $40.75 © 2008 American Chemical Society
Published on Web 01/19/2008

Table 1. $KOs_2O_6 \cdot nH_2O$ Phase Synthesis Conditions, Cell Parameters, and Superconducting Transition Temperature T_c

sample	sample description	washing agent	drying temperature and conditions	a (Å) (XRD at 298 K)	T_c (K)
A	hydrated 1	stirred with water, 1 h	298 K air	10.1202(12)	9.8(1)
B	hydrated 2 (neutron sample)	stirred with water, 30 min	350 K in air	10.1106(3)[a]	10.0(1)
C	part hydrated	stirred with DMF, quick water washing on filtering	298 K air 598 K/N_2	10.08825(17)	10.1(1)
D	dried; exposed to air and dried at 573 K	not washed	598 K/N_2	10.0828(12)	10.2(1)
E	dry box	not washed		10.0795(2)	10.2(1)

[a] PND.

preliminary room temperature investigations of the cesium and rubidium osmate β-pyrochlores also show large ADPs for the A site cation, although not as enlarged as that in KOs_2O_6. The structure of $RbOs_2O_6$ has also recently been studied as a function of temperature using neutron powder diffraction,[14] but while showing unusual behavior in the ADPs of the rubidium ion, this material shows no change in cell symmetry as a function of temperature.

Very recent work by Hiroi[15–17] on KOs_2O_6 has shown a different phase transition, of first order, at $T_p = 7.5$ K in the superconducting state in zero magnetic field. It was suggested that the transition is associated with the rattling of K^+ located in an anharmonic potential created by the Os-O units even if the influence of rattling and its transition on the superconductivity was not clear; this transition can have, presumably, a structural origin but neither symmetry change nor cell doubling was detected. However, it has been found that the intensity of some reflections changed slightly at the transition.[16]

The β pyrochlore structure is well known for a number of other metals occupying the B-type sites, for example, $ANbTeO_6$ and $ATaWO_6$ with A = K, Rb, Cs, and NaW_2O_6. In these materials the ability of the potassium and sodium based materials to reversibly absorb water into the pyrochlore channels is well documented. Thus for $KTaWO_6$ up to one water molecule may be absorbed reversibly to produce $KTaWO_6 \cdot H_2O$.[18,19] The structures of a number of materials of this type have been studied and of note is the work of Barnes et al. [20] on $KNbWO_6$ who investigated the structural changes that occur as water is absorbed, including studies as a function of pressure. In these $KTaWO_6 \cdot nH_2O$ materials as n increases the potassium ions become displaced to the 16d site with water molecules occupying 32e sites and coordinated to the potassium ions. In $NaW_2O_6 \cdot nH_2O$ a similar structural model has been determined with the sodium ion 7-coordinate to framework oxygen and the oxygen of the water molecule present in the pyrochlore channels.[21]

The sensitivity of the osmate pyrochlores to water is also alluded to in the literature. Despite this, methods of producing pure bulk polycrystalline material have involved washing with water to remove the commonly formed $AOsO_4$, A = K, Rb, Cs, impurities, followed by drying at 323–373 K. Furthermore single crystals have often been handled in air allowing for incorporation of water at least into the surface of the material. In this paper we report the effect of water incorporation into the KOs_2O_6 both on the structure and on the superconducting properties.

Experimental Section

Polycrystalline KOs_2O_6 was prepared by reaction of appropriate quantities of high-purity oxide OsO_2 (0.862g, Alfa Aesar, 99.99%) and of KO_2 (0.138 g, Aldrich). These materials were ground together thoroughly in a dry box, pressed into a pellet, and placed into a silica ampoule together with a small gold tube containing 0.13 g of Ag_2O to create an oxidizing atmosphere. The ampoule was sealed under vacuum, heated to 723 K at a rate of 100 K h^{-1}, and maintained at this temperature for 16 h before furnace cooling. Bulk, polycrystalline KOs_2O_6 synthesized at 723 K has been found to be purer than samples synthesised at lower temperature (623–703 K), while attempts to obtain material at higher temperatures were less successful as only the phases $KOsO_4$, OsO_2, and Os were detected as products.

Bulk KOs_2O_6 can be reliably synthesized using this method, but is not single phase and contains small amounts of OsO_2 (~5%), $KOsO_4$ (~20%), and OsO_4 (visibly observed as coating the wall of the tube and some crystallites). OsO_4 evaporates rapidly from the product at room temperature in a stream of air (Caution: OsO_4 is very toxic by inhalation, ingestion, or skin contact). $AOsO_4$ phases, A = K, Rb, Os, can be removed by washing with water or other polar solvents. Various alternative washing regimes were used in this study as summarized in Table 1 including the use of DMF (dimethylformamide) which dissolves $KOsO_4$ while also having a molecular diameter too large to enter the pyrochlore structure. A sample (sample **E**), consisting of a mixture of phases, was studied "as-made"; for this sample all handling was undertaken in strictly dry conditions (N_2 glovebox < 2 ppm H_2O) with the sealed reaction tube opened in the dry box.

X-ray diffraction patterns for all samples were collected at room temperature using a Siemens D5000 diffractometer, operating with a primary monochromator $\lambda = 1.54056$ Å, over a 2θ range of 10–110° with a step size of 0.02° over 15 h under dried nitrogen. Profiles indicated that for all the washed samples the main observed peaks could be indexed using a cubic cell with $a \sim 10$ Å with the space group $Fd\bar{3}m$; a few very weak peaks $I/I_0 < 0.04$ could be assigned to OsO_2. Accurate lattice parameters were obtained by

(13) Kuneš, J.; Pickett, W. E. *Physica B: Condens. Matter* **2006**, *378*, 898.
(14) Galati, R.; Hughes, R. W.; Knee, C. S.; Henry, P. F.; Weller, M. T. *J. Mater. Chem.* **2007**, *17*, 160.
(15) Hiroi, Z.; Yonezawa, S.; Yamaura, J. *J. Phys., Condens. Matter* **2007**, *19*, 145283.
(16) Sasai, K.; Hirota, K.; Nagao, Y.; Yonezawa, S.; Hiroi, Z. *J. Phys. Soc. Jpn.* **2007**, *76*, 104603.
(17) Hiroi, Z.; Yonezawa, S.; Nagao, Y.; Yamaura, J. *Phys. Rev. B: Condens. Matter* **2007**, *76*, 014523.
(18) Darriet, B.; Rat, M.; Galy, J.; Hagenmuller, P. *Mater. Res. Bull.* **1971**, *6*, 1305.
(19) Murphy, D. W.; Cava, R. J.; Rhyne, K.; Roth, R. S.; Santoro, A.; Zahurak, S. M.; Dyke, J. L. *Solid State Ionics* **1986**, *18−19*, 799.
(20) Barnes, P. W.; Woodward, P. M.; Lee, Y.; Vogt, T.; Hriljac, J. A. *J. Am. Chem. Soc.* **2003**, *125*, 4572.
(21) Thorogood, G. J.; Kennedy, B. J.; Luca, V. *Physica B: Condens. Matter.* **2006**, *385*, 91.

fitting the profile with GSAS[22] using the standard crystallographic description of the pyrochlore structure and varying only the profile parameters. For the unwashed samples additional peaks from $KOsO_4$ were observed in profile and accurate lattice parameters for the pyrochlore phase present in these materials were again extracted using profile fitting, with a second phase added to the modeling process to account for the $KOsO_4$ phase reflections.

A 3g sample was obtained by combining the products from several syntheses under identical conditions and using a washing scheme equivalent to that of sample **B**, and this was used for powder neutron diffraction studies. Neutron diffraction data were recorded on the high flux D20 diffractometer at the Institut Laue-Langevin, Grenoble, in the 2–500 K temperature range using a cryofurnace. Data were collected in the 2θ =10–150° range with a wavelength λ = 1.868 Å; a continuous ramp rate of 1 K min^{-1} was used. A longer period, 1 h, data set was collected initially at 2 K data. The sample was loosely sealed inside a vanadium can with a small header space. Data were also collected for an anhydrous polycrystalline sample of KOs_2O_6, and the detailed analyses of these will be reported elsewhere.

X-ray diffraction patterns at variable temperature were performed using a Bruker D8 diffractometer (λ = 1.5406 Å) under a flow of dry N_2. Data sets were collected every 10° C, on heating and cooling, in the temperature range 30–300 °C.

Magnetic and superconductivity data was collected using an Oxfords Instruments 3001 vibrating sample magnometer (VSM) with a 12 T superconducting magnet. Data was collected through the superconducting transition of the material over a temperature range of 14−2 K using a cooling rate of ~1 K/min under an applied field of 100 Gauss. Data was collected every 2 s and stored for analysis.

Thermogravimetric analysis (TGA) was performed to monitor the degree of hydration of samples of type **B** and **C**, using a TG-DSC NETZSCH STA 409 PC Luxx simultaneous thermal analyzer. The samples were placed in an alumina crucible and heated from room temperature to temperatures up to 800 K with a heating rate of 5 °C/min under a flow of argon; in some cases the samples were held at 800 K for 30 minutes prior to cooling to room temperature.

Results

Structure Analysis. Analysis of the various powder diffraction data sets was undertaken by the Rietveld method using the GSAS[22] program; this program also allows the rapid analysis of a large number of variable temperature data sets using the SEQGSAS option.[22] Initial analysis of the powder neutron diffraction data collected from sample **B** ($KOs_2O_6 \cdot nH_2O$) used the standard coordinate description for the β-pyrochlore structure in $Fd\bar{3}m$ with Os (0, 0, 0), A ($^3/_8$, $^3/_8$, $^3/_8$), and O (x, $^1/_8$, $^1/_8$). Single crystal X-ray diffraction studies on KOs_2O_6 were carried out by Schuck et al.,[9] according to which Bragg peaks violate $Fd\bar{3}m$ symmetry between 100 K and 400 K and structure becomes *non-centrosymmetric* with space group $F4\bar{3}m$. Inspection of the data collected from $KOs_2O_6 \cdot nH_2O$ at 2 K and at all other temperatures showed no measurable intensity associated with the (002), (024), or (006) reflections, see, for example, Figure 2, supporting the $Fd\bar{3}m$ description rather than $F4\bar{3}m$ for this hydrated material. However, it should be noted that these additional reflections in $F4\bar{3}m$ are weak and, despite the greater sensitivity of the neutron technique, the lower symmetry space group cannot be entirely ruled out.

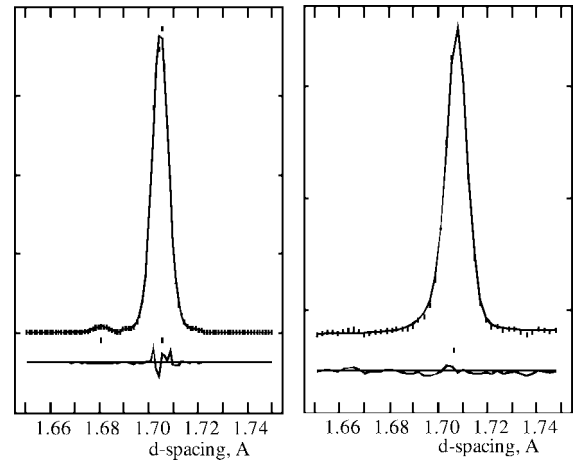

Figure 2. Calculated, left, using Schuck's $F\bar{4}3m$ model, and observed, right 2 K, profiles for $KOs_2O_6 \cdot nH_2O$ between 1.65 and 1.75 Å for D20. The calculated profile shows the (600) reflection at 1.6806 Å which is not visible in the experimental data from the hydrated $KOs_2O_6 \cdot nH_2O$ phase.

An initial refinement of the structure using the 2 K data converged rapidly using the simple $Fd\bar{3}m$ KOs_2O_6 crystallographic model; cell parameters, peak shape profiles, atomic positions, and ADPs were sequentially added to the refinement which converged smoothly to yield acceptable R factors (R_{wp}=3.95 %, R_p=2.81 %, χ^2 = 4.34). This model was then used as a basis for a SEQGSAS analysis of the remaining data sets from the temperature range 2–500 K. Preliminary analysis of the data extracted from the variable temperature range centered on the extracted lattice parameter, the potassium site ADP, and the background. Figure 3a summarizes the variation in lattice parameter between 2 and 500 K; between 2 and 350 K a normal monotonic increase in the a lattice parameter is observed before a significant drop between 350 and 450 K after which the cubic cell parameter starts to increase again. This drop in cell parameter was associated with a significant decrease in the background level (and also decreases in the extracted ADPs associated with the potassium site in this model, Figure 3b, indicating that some structural process occurs that involves this ion). The former is indicative of a decrease in hydrogen content in the material and reduction of the large incoherent scattering associated with this isotope. A likely explanation of these behaviors, particularly when associated with the TGA, vide infra, is that water is lost from the pyrochlore channels between 350 and 450 K and the correct description of the washed osmate pyrochlore, in the temperature interval below 350 K, is $KOs_2O_6 \cdot nH_2O$, on the basis of the TGA of sample $n \sim 0.1$. Therefore a new structural model was constructed to represent the hydrated phase.

Previous work on hydrated beta pyrochlores indicated that as water enters the structure the potassium ion shifts from the 8b site to the 16d site with the water oxygen position at 32e with $x \sim 0.42$. The 2 K powder neutron diffraction data were analyzed further with this model in mind. Structure refinements were undertaken with just the osmate octahedra portion of the structure description and difference Fourier maps calculated to determine the scattering density within

(22) Larson, A. C.; Von Dreele, R. B. *Generalised Structure and Analysis System*; Los Alamos National Laboratory: Los Alamos, NM, 1990.

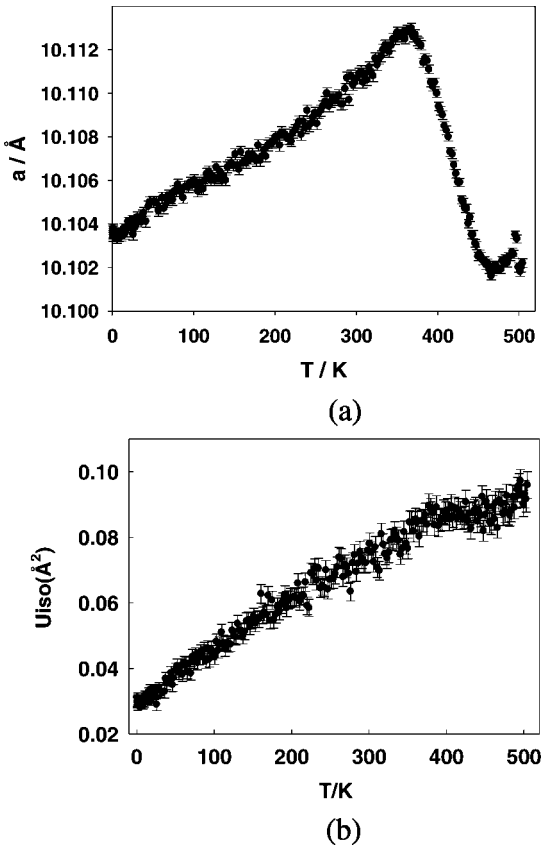

Figure 3. (a) Lattice parameter, a (Å), as a function of temperature as determined from profile fitting of the neutron powder diffraction data. Estimated standard deviations are shown as bars. (b) Variation in extracted potassium ADP as a function of temperature. Both figures related to the structure refinement using the simple β-pyrochlore based structure of KOs_2O_6.

the pyrochlore channels around the 16d and 8b sites. Possible sites for the missing scattering density were found, as expected at the 8b site, with weaker features at adjacent 32e sites ($x \sim 0.32$) and around the 16d position. Therefore a model was constructed with potassium allowed to occupy both the 8b and 16d sites (with the total model potassium level constrained to produce KOs_2O_6 with water oxygen introduced to 32e sites at (0.32, 0.32, 0.32) again with the overall site occupancy constrained to be equal to the level of potassium displaced from the adjacent 8b site. No attempt was made to included hydrogen atom positions because of the low water content and small hydrogen neutron scattering length. This model is similar to that used by Barnes et al. to describe hydrated phases in the $ANbWO_6 \cdot nH_2O$, A = K, Rb, systems[20] and reflects the likely structural changes that occur when water enters the structure when it occupies a site close to the original potassium site (8b), displacing a portion of it to a position close to the 16d site. To reduce the number of refinable variables in the Rietveld analysis and allow stable refinement, the displaced potassium was fixed on the 16d site at ($^1/_2$, $^1/_2$, $^1/_2$), and its ADP (U_{iso}) was also fixed at 0.08 Å^2. Given the proximity of the potassium ion on the 8b sites and the oxygen on the 32e site ($x \sim 0.32$) these atoms were constrained to have the same ADP. All other positional parameters and thermal parameters were varied. The refinement converged satisfactorily giving the structure description for $KOs_2O_6 \cdot nH_2O$ summarized in Table 2a,b; the extracted fit factors were $R_{wp} = 3.82$ %, $R_p = 2.71\%$, and $\chi^2 = 4.07$, showing a small improvement over the simple β-pyrochlore model originally used and further supporting this more realistic structure model, though there was a small increase in the number of crystallographic variables. Figure 4 shows the profile fits achieved using the simple β-pyrochlore model and the improved model with water oxygen and partially displaced potassium. The refined level of water oxygen produces a stoichiometry of $KOs_2O_6 \cdot nH_2O$ with $n = 0.08$, in good agreement with that determined from TGA of this material from which $n \approx 0.11$ (vide infra). Figure 5 shows a representation of this hydrated structure.

This structural model was then used in the SEQGSAS refinement to analyze the full temperature range of data from 2 K to 350 K. The model allowed the fractional occupancy of the water oxygen site to vary freely with concomitant and linked variations in the potassium levels on the 8b and 16d sites. For data sets collected above ~380 K this model showed a decrease in potassium level on the 16d site (and linked water oxygen on the 32e site) with the site occupancy falling from 0.040(6) at 350 K to 0.000(6) at 450 K. The potassium site occupancy on the 8b site increased towards unity in line with this change; see Figure 6 (note that while some refined site occupancy values above 350 K slightly exceeded unity they were within one estimated standard deviation). This represents the expected loss of water from the structure and transfer of potassium from the 16d to the 8b site. Once water is fully lost from the structure the crystallographic description effectively reverts to one with full occupancy of the 8b site by potassium, which is the normal β pyrochlore description, and such a model was suitable for the analyses of the remainder of the variable temperature data sets from 460 to 500 K. Note that while single crystal data for as-prepared, anhydrous KOs_2O_6[9,10] indicates a cell symmetry of $F\bar{4}3m$, our data at 450 K and above from dehydrated $KOs_2O_6 \cdot nH_2O$ show no evidence for this crystallographic description. However, it is unlikely that we would be able to distinguish the two models because of the large thermal motion of the potassium ions at these temperatures and only insignificant differences in the diffraction intensities. Figures 7a−e summarizes the key extracted structural information from the variable temperature powder neutron diffraction study using the model.

TGA. TGA scans on two hydrated samples, **A** and **C**, shown in Figure 8, prove that the mass losses between 323 K and 523 K during heating are 0.42% and 0.17%, respectively. The fully hydrated sample, **A**, shows a further sharp increase in mass loss starting at around 530 K while for the partially hydrated sample a similar weight loss occurs starting around 573 K. These large additional weight losses could have a number of origins. Residual volatiles trapped within the samples such as OsO_4 or $KOsO_4$ may be evolved or more likely it is due to decomposition of the pyrochlore phase through loss of potassium oxides or disproportionation and loss of OsO_4. Extra peaks that appear in the powder X-ray diffraction patterns of samples repeatedly heated to above 500 K and which occur with simultaneous broadening and weakening of the pyrochlore reflections, confirm this

Table 2. (a) 2 K Structural Model for $KOs_2O_6 \cdot 0.08H_2O$[a] and (b) Key Derived Bond Distances (Å) and Angles (deg) in $KOs_2O_6 \cdot 0.08H_2O$[b]

(a) Structural Model

name/site	*x*	*y*	*z*	$U_i/U_e \times 100$ (Å^2)	site occupancy
K1 8b	$^3/_8$	$^3/_8$	$^3/_8$	2.22(10)	0.924(11)
Os 16d	0	0	0	0.10(2)	1.0000
OW 32e	0.326(7)	0.326(7)	0.326(7)	2.22(10)	0.022(3)
O1 48f	0.31715(11)	$^1/_8$	$^1/_8$	0.51(5)	1.0000
K2 16d	$^1/_2$	$^1/_2$	$^1/_2$	8.00	0.038(6)

(b) Bond Distances and Angles

atoms	multiplicity	bond length/bond angle
K1−O1	× 6	3.1104(11)
K1−O1	× 12	3.61968(19)
Os−O1	× 6	1.9106(4)
O1−Os−O1	× 3	91.86(4)
O1−Os−O1	× 3	88.14(4)
K2−O1	× 6	2.5697(8)
K2−OW	× 6 (both sites occupied at low levels)	2.067(7)

[a] Space group $Fd\bar{3}m$, $a = 10.10363(19)$ Å, $V = 1031.41(3)$ Å^3. [b] Estimated standard deviations in parentheses.

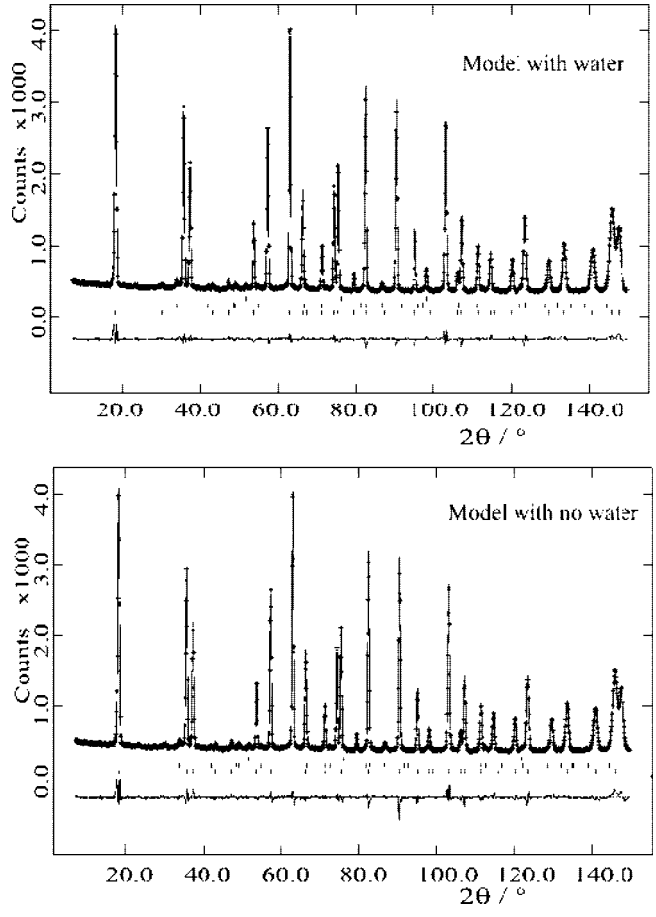

Figure 4. Upper: profile fit achieved using the model summarized in Table 2a. Lower: the poorer profile fit to the same experimental data using the simple β-pyrochlore structure description. Crosses are observed data, upper continuous line is the calculated profile, and lower continuous line is the difference. Tick marks show the reflection positions.

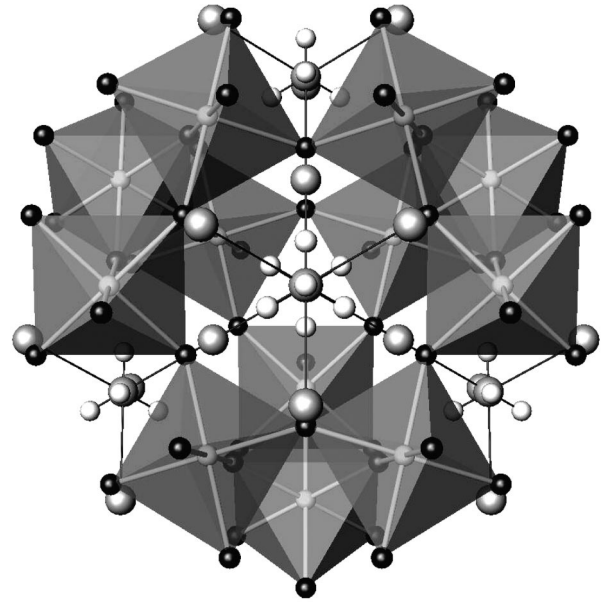

Figure 5. β-Pyrochlore based structure of $KOs_2O_6 \cdot nH_2O$ showing the partially displaced potassium ions and associated water oxygen position, shading scheme as Figure 1.

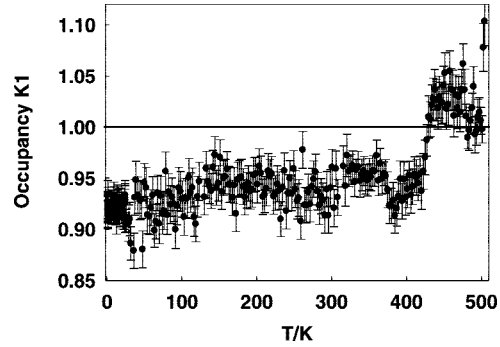

Figure 6. Variation as a function of temperature in the refined site occupancy parameter for the K1, 8b, position. Estimated standard deviations are shown as error bars.

decomposition. Considering just the mass loss between 323 and 530 K, which corresponds to the temperature range where significant changes in the lattice parameter occur in both X-ray and neutron diffraction data, the water content in the structure for the fully hydrated sample corresponds to 0.11 mol, that is, $KOs_2O_6 \cdot 0.11H_2O$, while for the partially hydrated sample it is around half of that amount. As already pointed out the former value is consistent with the stoichiometry obtained from the refined site occupancy factors of the similar sample used in the NPD analysis, though the instability of the phases seen on heating further above 530 K, in flowing argon, means that the values should be treated with some caution.

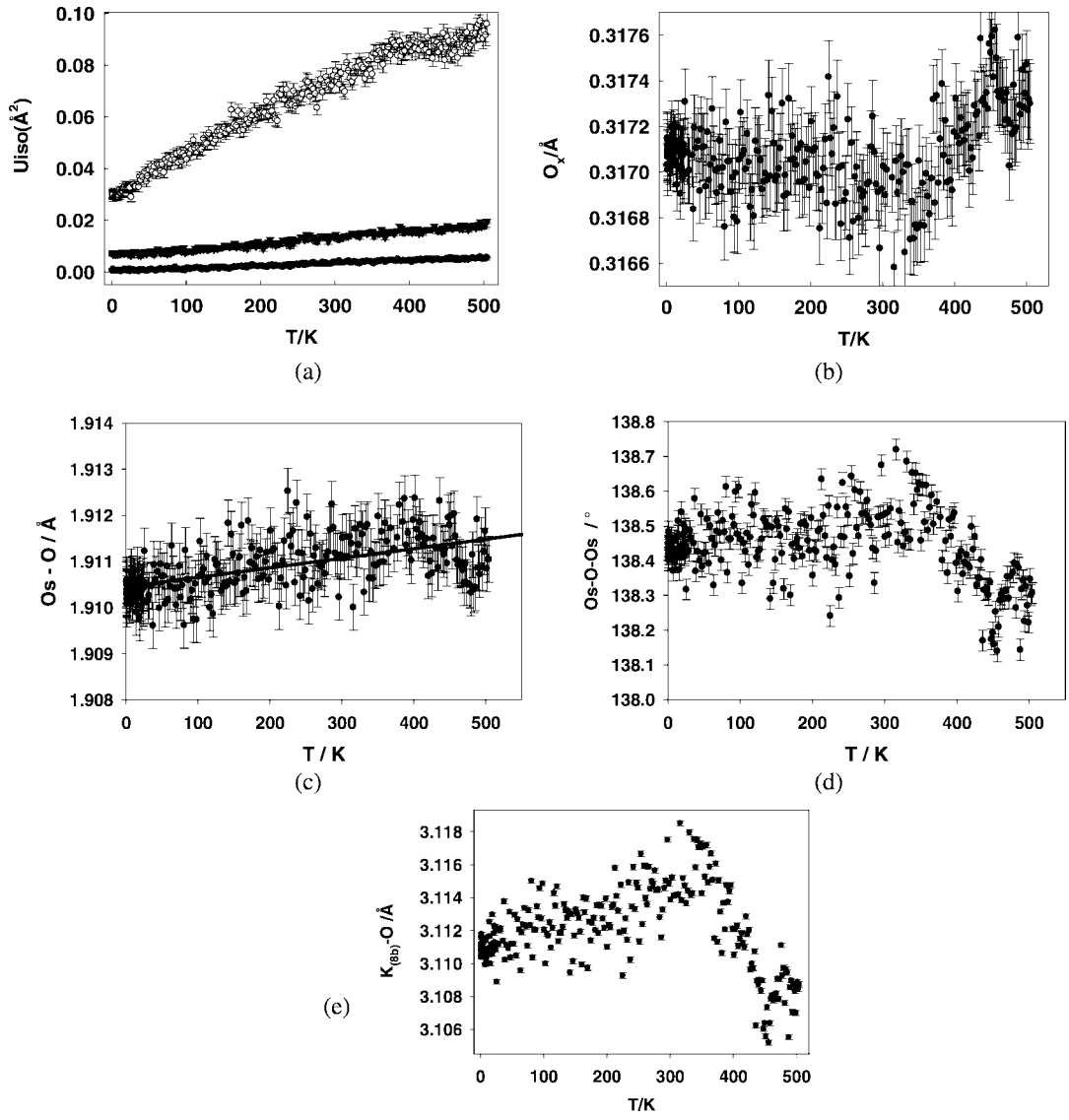

Figure 7. a−e. Variation of various structural parameters as a function of temperature: (a) U_{iso} (Å^2) ADPs for K1 (○), Os (●) and O1(▼); (b) framework oxygen (O1) x coordinate, (c) Os−O1 distance, (d) Os−O1−Os bond angle, and (e) K1−O1 distance.

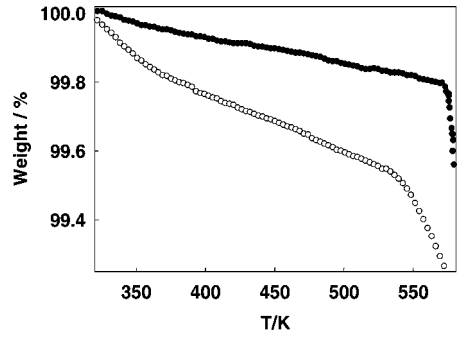

Figure 8. TGA data for the fully hydrated (sample **A**, ○) and partially hydrated KOs_2O_6 (sample **C**, ●).

Superconducting Properties. VSM data were collected for all samples, **A**−**E**; Figure 9 shows data from key samples over the lowest temperature portion where the materials become superconducting. The data appear to show a correlation between the level of hydration and the superconducting transition of the material, with T_c lowering as more water is incorporated into the structure. Determined onset T_c's for **A**, **C**, and **D** were 9.8(1) K, 10.1(1) K, and 10.2(1) K, respectively.

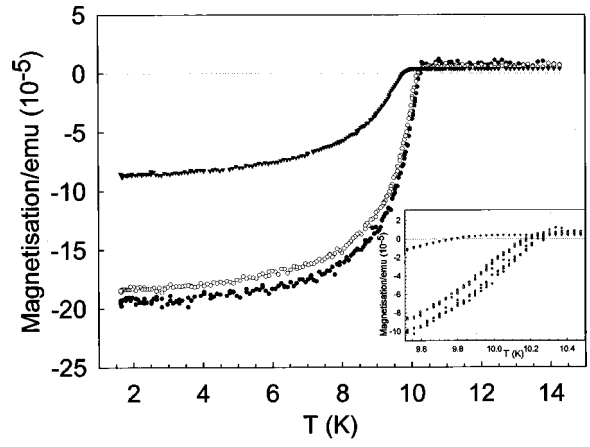

Figure 9. Overall magnetization of the materials for **D** (dried, ●), C (stirred with DMF and washed briefly with water, ○) and A (fully hydrated, ▼) samples. Inset: expanded view around 10 K.

Variable Temperature X-ray Analysis in an Open System. Powder X-ray diffraction data sets were collected from sample **C**. These were fitted in a similar method to the neutron diffraction data sets using SEQGSAS, but because

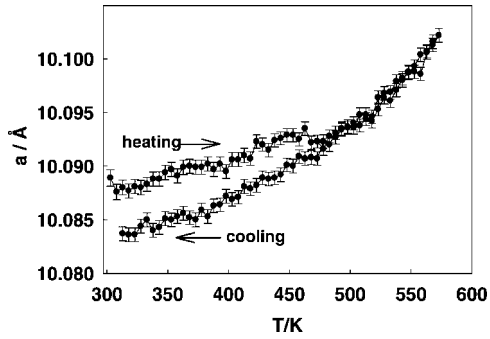

Figure 10. Lattice parameter of $KOs_2O_6 \cdot nH_2O$, $n \sim 0.1$, samples as a function of temperature from powder X-ray diffraction as a function of heating and cooling in flowing N_2.

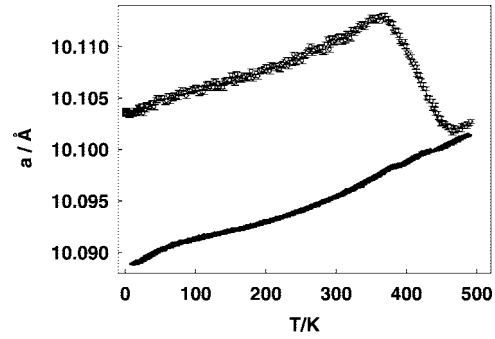

Figure 11. Comparison of the lattice parameter variation of hydrated $KOs_2O_6 \cdot 0.11H_2O$ and anhydrous KOs_2O_6 as a function of temperature between 2 K and 550 K from powder neutron diffraction data.

of the insensitivity of the X-ray method to potassium and oxygen in this system just a simple osmate framework model in $Fd\bar{3}m$ was used to fit the data and extract the variation of the lattice parameter as a function of temperature on both heating and cooling cycles between 298 and 580 K, Figure 10. Values obtained on heating showed similar variation as seen with the powder neutron diffraction data with a lattice parameter contraction centered around 450 K. On cooling the lattice parameter of the thermally dehydrated phase contracts producing a room temperature value significantly smaller than the hydrated starting material and consistent with the value of an anhydrous as-prepared KOs_2O_6 phase, sample **E**.

Discussion

The observed increase in lattice parameter on washing potassium osmate pyrochlores with water reflects the incorporation of water into the pyrochlore channels. The magnitude of this increase of 0.04 Å is smaller than that observed in other potassium β pyrochlores, for example, $KNbWO_6$, where the lattice parameter increases by around 0.20 Å for the addition of 1 mol of water into the material. This reflects only partial hydration in the osmate materials. Washing the samples in DMF alone produced no increase in lattice constant, consistent with this observation. The hydration−dehydration process is initially fully reversible though cycling around this process by repeatedly heating to above 575 K was found to result in slow degradation of the material with loss of crystallinity and appearance of additional phases. Thus comparison of variable temperature powder neutron diffraction data from the hydrated phase and an anhydrous phase, Figure 11, shows that once the material is fully dehydrated the lattice parameter reverts to that of a heated sample of anhydrous KOs_2O_6.

The mode of incorporation of water into the superconducting potassium osmate pyrochlores parallels that seen in other β-pyrochlores. That is, as water is inserted into the pyrochlore channels it displaces the potassium ion from the 8b site to the 16d site. Derived bond lengths and angles, Table 2b, are consistent with this description, with potassium to osmate framework oxygen distances decreasing in length as potassium shifts to the 16d site. In the $KOs_2O_6 \cdot 0.11H_2O$ system the cation-shift mechanism seems to occur only in part, limiting the level of water incorporated. The origin of this effect is unclear and attempts to further increase the water content through; for example, extended periods of stirring with water produces materials with a maximum water content of n, in $KOs_2O_6 \cdot nH_2O$, approaching 0.2, and results in increasing sample degradation. This may reflect the ease with which osmium (5.5+) can be reduced, thus undergoing a slow redox reaction with water. Another effect might be the smaller lattice parameter of the KOs_2O_6 ($a \sim 10.1$ Å) system compared with $KTaWO_6$ ($a \approx 10.3$ Å) impeding water molecule and potassium ion diffusion along the pyrochlore channels. Indeed comparison of the various potassium β-pyrochlores that form fully hydrated phases $AB_2X_6 \cdot H_2O$ show that hydration is limited to those with large lattice parameters for the anhydrous material; thus, K(Ta,Nb)WO_6 and $KNiCrF_6$ ($a = 10.24$ Å)[23] form a hydrated $KNiCrF_6 \cdot H_2O$ ($a = 10.45$Å),[24] but for phases such as $K(Ti_{0.5}Te_{1.5})O_6$ ($a =$ 10.06 Å),[25] hydrated phases are unknown.

When water does enter the β-pyrochlore structure it is accommodated in the larger cavities surrounding the 8b site. However, this position is originally fully occupied by potassium though the site is effectively larger than that required by the ionic radius and coordination demands of this ion. Thus the ion may be locally displaced or show high anisotropic ADPs associated with the ion "rattling".[10–12] Even so there is insufficient room for the water molecule to share this 8b centered cavity with a potassium ion, and a proportionate level of potassium is displaced to the 16d site to accommodate the inserted water.

The thermal variations of key positional, bond length, angle, and ADPs are summarized in Figure 7a−e. The framework oxygen, O1, x coordinate is the only variable, in combination with the lattice parameter, that defines the geometry of the osmium−oxygen framework and the potassium−oxygen distances of the standard $Fd\bar{3}m$ beta pyrochlore description. Between 2 K and 350 K for $KOs_2O_6 \cdot 0.08H_2O$ this x-coordinate is almost invariant showing only a small, insignificant, within estimated standard deviations, decrease which translates, in combination with the increase in lattice parameter over this temperature range, into the expected small increase in the Os−O distance (Figure

(23) Babel, D. *Zeit. Anorg. Allg. Chem.* **1972**, *387*, 161.
(24) Babel, D.; Pausewang, G.; Viebahn, W. *Z. Naturforsch., B: Anorg. Chem. Org. Chem.* **1967**, *22*, 1219.
(25) Castro, A.; Rasines, I.; Turrillas, X. M. *J. Solid State Chem.* **1989**, *80*, 227.

7c) and the derived Os−O−Os bond angle (Figure 7d) as the material expands. Between 350 and 450 K there is a marked increase in the O1 *x* coordinate which occurs at the same time that the lattice contracts when water is lost from the structure. The Os−O1 distance is almost invariant over this temperature range, but the Os−O−Os bond angle becomes significantly more acute as the OsO_6 octahedra tilt allowing the structure to contract and coordinate more strongly to the potassium ion on the K1 site (Figure 7e). This behavior is also reflected in the potassium ion ADP which plateaus in this region presumably as a result of an associated decrease in the volume of the local coordination site. Above 450 K the dry KOs_2O_6 material starts to demonstrate normal expansion of the pyrochlore framework with the Os−O and K1−O1 distances and the Os−O−Os angle all increasing as a function of temperature.

The effect on the superconducting properties in the $KOs_2O_6 \cdot nH_2O$ system seems to be a slight degradation in both T_c and superconducting volume. Thus T_c falls from 10.2 K in totally dry materials to 9.8 K for $KOs_2O_6 \cdot nH_2O$ ($n \approx 0.2$). Interestingly, the value for our anhydrous polycrystalline material, handled totally in the absence of moisture (sample **E**), is slightly higher than previously reported values for KOs_2O_6 (Table 1). The decrease in T_c as water is inserted could have two compositional/structural origins. Firstly incorporation of water results in a small increase in lattice parameter, and the value of T_c shows an inverse correlation with lattice constant in the series AOs_2O_6, A = Cs, Rb, K. Alternatively the "rattling" of the smallest potassium ions on the 8b sites has been proposed as a reason for the highest T_c value for this osmate derivative in the series A = K, Rb, Cs. That is, low lying phonons are associated with the rattling potassium ion located in a highly anharmonic potential, and these give rise to anomalous electron scattering and strong-coupling superconductivity.[17] Incorporation of water into the KOs_2O_6 structure will affect the rattling of potassium ions/nature of the low lying phonons as a result of both the displacement of the potassium ions and the partial occupation of the normal potassium ion sites by water molecules. By quenching a number of the low-energy phonons a decrease in T_c might be expected in such a strongly coupled superconductor.[16]

Finally, we see no evidence for reduction in symmetry from $Fd\bar{3}m$ to $F4\bar{3}m$ in $KOs_2O_6 \cdot nH_2O$. Schuck et al.[10] maintain that their anhydrous KOs_2O_6 samples show evidence of symmetry breaking to $F4\bar{3}m$ in high intensity single crystal X-ray diffraction studies while Hiroi et al. find no evidence of such behavior in their single crystals.[16] We too see no evidence of a reduction from $Fd\bar{3}m$ symmetry in our anhydrous polycrystalline materials but disordered displacements of potassium ions within the pyrochlore cavity that can be fully modeled in $Fd\bar{3}m$. It is possible that differences in preparative methods may be the origin of these results. In our partially hydrated samples further disorder results from the partial incorporation of water and the formation of an "averaged" structure consisting of hydrated and anhydrous domains; again this can be modeled well in $Fd\bar{3}m$. The sensitivity of KOs_2O_6 to water uptake should be noted, and it is likely that single crystals as well as polycrystalline material will rapidly take up some water into their surface layers even in moist air. This may affect the measured properties and the determined structures of KOs_2O_6 phases unless water has been scrupulously avoided.

Acknowledgment. We thank EPSRC for support for this work under Grant EP/D00386 and the ILL for the provision of neutron beam time (Expt 5-24-270).

CM702972C